Journal of Alloys and Compounds 484 (2009) 390–394

Contents lists available at ScienceDirect

Journal of Alloys and Compounds

journal homepage: www.elsevier.com/locate/jallcom

Effect of graphite flake on microstructure as well as mechanical properties and thermal shock resistance of ZrB_2–SiC matrix ultrahigh temperature ceramics

Zhi Wang*, Sai Wang, Xinghong Zhang, Ping Hu, Wenbo Han, Changqing Hong

Center for Composite Materials, Harbin Institute of Technology, Harbin 150001, China

ARTICLE INFO

Article history:
Received 3 March 2009
Received in revised form 21 April 2009
Accepted 22 April 2009
Available online 3 May 2009

Keywords:
Zirconium diboride
Ceramics
Microstructure
Mechanical properties

ABSTRACT

ZrB_2–20vol.%SiC containing the various volume fractions of graphite flake (ZSG) composites were investigated to determine the effect of graphite content on the microstructure as well as the mechanical properties and thermal shock resistance. The results revealed that the flexural strength generally decreased as the graphite volume fractions increased. Compared with the fracture toughness of about 4.5 MPa $m^{1/2}$ for the ZrB_2–SiC composites, the toughness of the ZSG composites is essentially higher than that of the ZrB_2–SiC composites due to their lower strength relative to the ZrB_2–SiC composites. The toughening mechanisms, such as the crack deflection and bridging, were related to the thermal residual stresses, and the thermal residual stresses in interfaces were calculated using Hsueh's formula. Moreover, the critical crack size that represents thermal shock resistance was calculated using the Griffith criterion. It was found that the thermal shock resistance was improved with the increasing graphite volume fractions.

1. Introduction

Zirconium diboride (ZrB_2) based ultrahigh temperature ceramic matrix composites are a leading candidate as potential materials for a variety of high temperature structural applications [1–7], such as furnace elements, plasma arc electrodes, hypersonic aircraft, reusable launch vehicles, or rocket engines and thermal protection structures for leading edge parts on hypersonic reentry space vehicles at over 1800 °C [1,2]. It is primarily because ZrB_2 has an excellent combination of mechanical, physical, chemical and oxidation resistance properties [1,2,8,9]. It is known that the addition of appropriate amounts of SiC particles not only enhances the mechanical properties [3,4,10], but also improves the oxidation resistance of ZrB_2 by promoting the formation of silicate-based glasses that inhibit oxidation at temperatures between 800 and 1700 °C [4,11]. Although the ZrB_2–SiC composites have many advantages, their intrinsic characteristics such as low fracture toughness (premature failure due to brittle fracture), low toughness induced poor thermal shock resistance are still obstacles for them to be used widely, especially for applications in extreme environment [12]. One possible route has been to overcome these deficiencies by incorporating the second phase additions with a higher aspect ratio (e.g., flakes or rods/whiskers) into the ZrB_2 based composites [13]. The graphite flake is an attractive material for high temperature applications due to its high strength, high modulus, layered structure that allows for self-lubrication, excellent thermal shock resistance, and high fracture toughness [14]. Our previous works have revealed that the introduction of graphite flake into the ZrB_2–SiC composites can not only increase fracture toughness can but also improve thermal shock resistance compared with the ZrB_2–SiC composites [15]. Nevertheless, our previous works are insufficient to investigate the effect of the graphite flake on the microstructure as well as the mechanical properties and thermal shock resistance of graphite toughened ZrB_2–SiC ultrahigh temperature ceramics.

In the present work, ZrB_2–20vol.%SiC containing the various volume fractions of the graphite flake (ZSG) composites were fabricated by hot-pressing. The effect of graphite content on the microstructure as well as the mechanical properties and thermal shock resistance of the ZSG composites was investigated in detail.

2. Experimental procedures

2.1. Materials' preparation

Commercially available ZrB_2 with a mean size of about 3 μm, SiC with a mean size of about 2 μm and graphite flake (mean diameter and thickness are 15 and 1.5 μm, respectively) were purchased from Alfa Aesar Co., Ltd., USA. Their reported purity was more than 98%. The powder mixtures of ZrB_2 plus 20vol.%SiC plus 10, or 15, or 20, or 30 vol.% graphite flake were ball mixed for 20 h in a polyethylene bottle using ZrO_2 balls and ethanol as the grinding media. Then they were labeled as ZSG10, ZSG15, ZSG20 and ZSG30, respectively. After mixing, the slurry was dried in a rotary evaporator and screened. The sintering parameters for four batches of powder mixtures were summarize in Table 1.

* Corresponding author. Tel.: +86 451 86402382; fax: +86 451 86402382.
E-mail address: wangzhi1780@126.com (Z. Wang).

0925-8388/$ – see front matter © 2009 Elsevier B.V. All rights reserved.
doi:10.1016/j.jallcom.2009.04.109

Table 1
Sintering parameters of the ZSG composites: *T*, temperature; *P*, pressure; *t*, time.

Materials	Temperature (°C)	Pressure (MPa)	Holding time (min)	Atmosphere
ZSG10	1900	30	60	Vacuum
ZSG15	1900	30	60	Vacuum
ZSG20	2000	30	60	Vacuum
ZSG30	2000	30	60	Vacuum

2.2. Characterization

The bulk density of each composition was measured using the Archimedes' technique with deionized water as the immersing medium. The relative density was determined by dividing the bulk density by the theoretical density based on a rule of mixture calculation. The microstructural features of the ZSG composites were observed by scanning electron microscopy (SEM, FEI Sirion, Holland) along with energy dispersive spectroscopy (EDS, EDAX Inc) for chemical analysis. Flexural strength (σ) was tested in three point bending on 3 mm by 4 mm by 36 mm bars, using a 30 mm span and a crosshead speed of 0.5 mm min^{-1}. Each specimen was ground and polished with diamond slurries down to a 1 μm finish. The edges of all the specimens were chamfered to minimize the effect of stress concentration due to machining flaws. Fracture toughness (K_{IC}) was determined by a single-edge notched beam test with a 16 mm span and a crosshead speed of 0.05 mm min^{-1} using 2 mm by 4 mm by 22 mm test bars, on the same jig used for the flexural strength. A minimum number of 10 specimens were tested for each composition and all specimens were cut from same billet. During mechanical properties testing, the tensile surface of all the specimens was perpendicular to the hot pressing axis.

3. Results and discussion

3.1. Microstructure

Fig. 1 shows typical SEM micrographs of the fracture surfaces of the ZSG composites. The results of EDS analysis demonstrated (not shown here) that the small darker phase is SiC and it appears to be uniformly dispersed in the lighter ZrB_2 matrix. The graphite flake was observed in the fracture surface and its size did not change compared with the raw graphite flake size. The microcracks within graphite flake were readily detected in the fracture surface of the ZSG composites and the amount of the microcracks increased with the increasing graphite volume fractions. Furthermore, a small quantity of closed pores was also observed in the fracture surface.

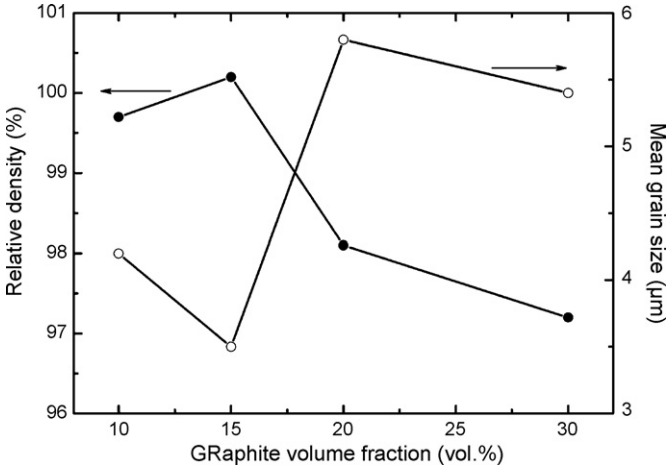

Fig. 2. Relative density and mean grain size of the ZSG composites.

The ZrB_2 grain sizes were determined from SEM images using an image analysis software package. The average grain size was estimated by measuring at least 120 grains. The ZrB_2 mean grain size for the ZSG composites is shown in Fig. 2. For the specimens sintered at temperature of 1900 °C, the ZrB_2 mean grain size decreased from 4.2 μm for ZSG10 composite to 3.5 μm for ZSG15 composite. The ZrB_2 mean grain sizes for ZSG20 and ZSG30 were significantly

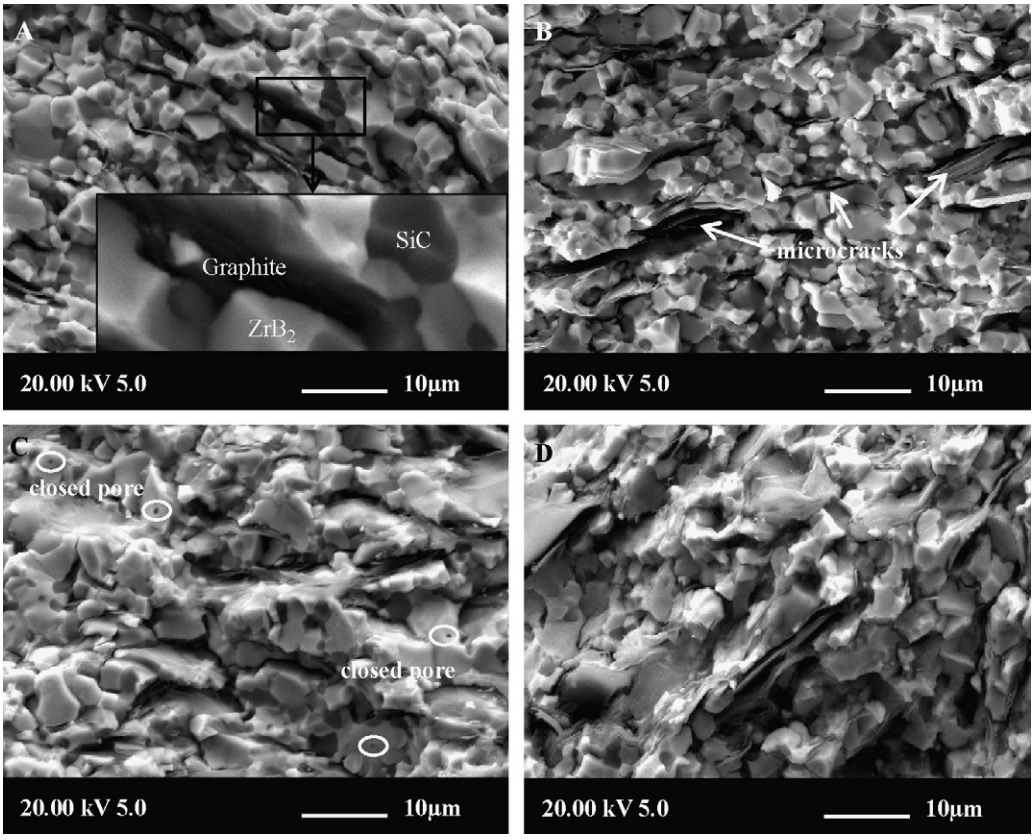

Fig. 1. SEM micrographs of fracture surface of the ZSG composites. Graphite volume fractions: A, B, C and D were 10 vol.%, 15 vol.%, 20 vol.% and 30 vol.%, respectively.

Table 2
Mechanical properties and critical crack size of the ZSG composites.

Materials	Flexural strength (MPa)	Fracture toughness (MPa $m^{1/2}$)	Critical crack size (μm)
ZSG10	490.77 ± 21.11	6.06 ± 0.21	152.95
ZSG15	480.96 ± 28.15	6.11 ± 0.24	162.03
ZSG20	367.77 ± 20.16	5.21 ± 0.18	201.53
ZSG30	277.06 ± 10.15	4.07 ± 0.15	215.88
ZrB_2–SiC [1,3,4]	>800	<5.0	<39.06

greater than that for ZSG10, which was because high sintering temperature resulted in coarsening of ZrB_2 grains. Likewise, the ZrB_2 mean grain size also decreased as the graphite volume fractions increased for the specimens sintered at temperature of 2000 °C. The grain coarsening in nonoxides ceramics, including diborides, is promoted by oxygen present as oxide impurities on the particle surfaces [13]. Therefore, the reduction in ZrB_2 mean grain size with increasing graphite volume fractions for the specimens sintered at same temperature was attributed to removal of oxide impurities due to reaction of oxide impurities with graphite (specific reactions are discussed below).

The relative density values of the ZSG composites are also shown in Fig. 2, which revealed that the relative densities increased from 99.7 to 100.2% as the graphite volume fractions increased from 10 to 15 vol.% and the further increase in graphite volume fractions to 30 vol.% led to the reduction in relative densities to 97.2%. Contrary to the well-known limitations of the densification behavior of ZrB_2-based composites [16], the obtainment of high dense bulk (>97%) was profited from the introduction of the graphite flake. The graphite substantially promoted densification of the ZSG composites by reacting with oxygen impurities which has been reported for other non-oxide ceramics such as TiB_2 [13,17]. It was recognized that the main impurities on the surface of ZrB_2 particles were ZrO_2 and B_2O_3. The impurity was SiO_2 on the surface of SiC particles. Furthermore, the impurity ZrO_2 was inevitably introduced into powder mixtures during ball milling. At elevated temperature, graphite reacted with ZrO_2 and B_2O_3 by the classic carbothermal reduction reaction, which was used to synthesize ZrB_2 commercially:

$$ZrO_2 + B_2O_3(l) + 5C = ZrB_2 + 5CO(g) \quad (1)$$

In the present work, a high vacuum (pressure 5 Pa) was maintained during hot-pressing. CO gas was readily removed by the vacuum, which was thermodynamically favorable to reaction (1). ZrO_2 and B_2O_3 on the surface of ZrB_2 were converted to very fine ZrB_2 particles and CO gas. The elevated temperature resulted in the evaporation of B_2O_3 liquid at 1450 °C under high vacuum [18], which led to excessive ZrO_2 based on the stoichiometry of reaction (1); then the residual ZrO_2 could react with graphite to produce ZrC according to reaction (2):

$$ZrO_2 + 3C = ZrC + 2CO(g) \quad (2)$$

Our previous work had demonstrated the existence of limited amounts of ZrC in the ZSG composites [19], which also indicated excessive ZrO_2. The impurity SiO_2 reacted with graphite to form SiC according to reaction (3):

$$SiO_2 + 3C = SiC + 2CO(g) \quad (3)$$

The increase in the densification from 99.7% for the ZSG10 to 100.2% for the ZSG15 composites was attributed to removal of oxide impurities because of their reactions with graphite [17,20]. Furthermore, the very fine ZrB_2, ZrC and SiC particles formed in situ on the surface of the ZrB_2 and SiC particles had a high sinterability, which also could provide a higher driving force for sintering because densification is driven by minimization of surface free energy. The higher driving force for sintering was also thought to be the main responsible for the increase in densification from 99.7% for ZSG10 to 100.2% for ZSG15 [13]. However, the graphite flake in the ZSG20 and ZSG30 composites was less dense and contained flaws in the form of microcracks, which resulted in the reduction in the relative densities. The high sintering temperature resulted in coarsening of ZrB_2 and SiC grains and the pore growth, which also caused the reduction in the relative densities.

3.2. Mechanical properties and thermal shock resistance

The flexural strength values of the ZSG composites are summarized in Table 2. The flexural strength generally decreased as graphite volume fractions increased. The reduction in flexural strength could be ascribed to the increase in weakening factors with increasing graphite volume fractions [19]. Furthermore, the strength of ZrB_2-based ceramics is reported to be strongly dependent upon the grain size. Therefore, the character and size of graphite flake (especially in the diameter direction, 10–20 μm) in this work limited the flexural strength compared with the ZrB_2–SiC composites [1,3,4]. The flexural strength values for ZSG10 and ZSG15 were statistically identical at 490 to 480 MPa, which was attributed to the grain refinement and the increase in the densification. The flexural strength decreased from 367 to 277 MPa as the graphite volume fractions increased from 20 to 30 vol.%. The significant reduction in the flexural strength was not only ascribed to the increase in weakening factors with graphite volume fractions, but also ascribed to grain coarsening and the reduction in the densification.

The fracture toughness values of the ZSG composites are also summarized in Table 2. The flexural strength of ZSG15 composite did not increase compared with one of ZSG10 composite, the slight increase in the fracture toughness from 6.06 to 6.11 MPa $m^{1/2}$ was thus attributed to the increase in toughening factors with increasing graphite volume fractions, namely, the crack deflection and branching as well as stress relaxation near the crack tip [3,19]. When graphite volume fractions were more than 15 vol.%, the fracture toughness decreased from 5.21 MPa $m^{1/2}$ for ZSG20 composite to 4.07 MPa $m^{1/2}$ for ZSG30 composite, which was due, primarily, to the reduction in the flexural strength because fracture toughness (K_{IC}) measured by a single-edge notched beam test strongly is dependent on the strength of materials [21]. Compared with the fracture toughness of about 4.5 MPa $m^{1/2}$ for the ZrB_2–SiC composites, the graphite addition of 10–20 vol.% significantly improved the toughness of the ZSG composites. For the ZSG30 composite, the fracture toughness of 4.07 MPa $m^{1/2}$ was numerically lower than that of the ZrB_2–SiC composites. The ZSG composites have essentially higher toughness than do the ZrB_2–SiC composites due to their lower strength relative to the ZrB_2–SiC composites. To understand the toughening mechanisms of the graphite flake, the specimens were indented using a load of 1.0 kg and SEM micrographs of the indentation cracks were described elsewhere [19]. The crack deflection and branching as well as bridging were observed near the interface between the graphite and other phases. It is believed that these interaction effects absorb crack propagation energy during fracture and lead to the improvement in toughness of the ZSG composites [22]. In addition, it should be noted that the

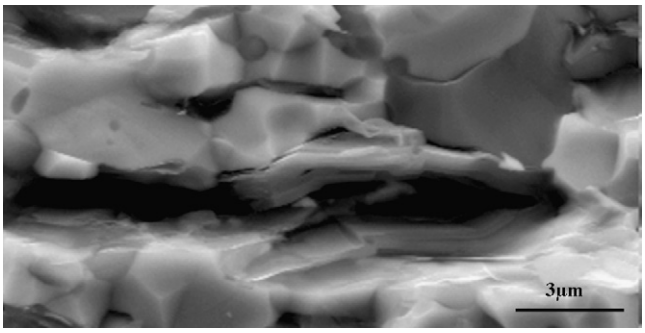

Fig. 3. SEM micrograph of the ZSG15 composite showing strain contours around graphite flake.

direct crack measurement was not a suitable technique to measure the toughness of the ZSG composites with lower hardness because the cracks did not propagate directly away from the corners of the hardness indentation. The crack propagation modes were related to the thermal expansion and elastic modulus mismatch between graphite flake and other phases in the ZSG composites. These mismatches would lead to a higher concentration of the residual stresses when the ZSG composites were cooled from the hot-pressing temperature (1900 or 2000 °C). The stress distribution around graphite flake was similar to that around whisker because the stress was perpendicular to interfaces between the graphite flake and other phases. Therefore, the thermal residual stresses could be evaluated using Hsueh's formula [23]:

$$\sigma_0 = \frac{(\alpha_m - \alpha_g)\Delta T}{\frac{1+\upsilon_m}{(1+\upsilon_g)E_m} + \frac{(1-2\upsilon_g)}{E_g}} \quad (4)$$

where σ_0 is the thermal residual stress, α is the thermal expansion coefficient, υ is the Poisson's ratio, E is Young's modulus, and ΔT is the temperature change (negative for cooling). The subscripts m and g refer to the matrix (ZrB_2 or SiC) and the graphite, respectively. For the ZSG composites, E_{ZrB2} = 490 GPa, E_{SiC} = 550 GPa, E_g = 15 GPa; υ_{ZrB2} = 0.17, υ_{SiC} = 0.14, υ_g = 0.25; $\alpha_{ZrB2} = 6.8 \times 10^{-6}$/K, $\alpha_{SiC} = 4.7 \times 10^{-6}$/K, $\alpha_g = 30 \times 10^{-6}$/K [2,15,24]. According to Hsueh's formula, the maximum thermal residual stresses at ZrB_2-graphite and SiC-graphite interfaces were evaluated to be about 1.3 and 1.4 GPa, respectively. The presence of the thermal residual stress was confirmed by SEM image, where strain contours were clear around graphite flake as shown in Fig. 3, and strain contours were parallel to graphite flake. When a crack propagates through the thermal residual stress field, its propagation energy could be dissipated and the crack was deflected or pinned. The thermal residual stress could also result in interfacial friction between graphite and other phases when the graphite flake was pulled out during crack propagation.

Improvement in toughness is valuable to improve the thermal shock resistance of ceramic matrix composites, and its reliability at ultrahigh temperature conditions [25], whereas, the reduction in the strength seems to degrade the thermal shock resistance based on Hasselman's theory. The literatures have reported that the ZSG composites have better thermal shock resistance than do the ZrB_2–SiC composites [15,26]. In order to further investigate the effect of the toughness and strength on the thermal shock resistance, the Griffith fracture criterion was applied based on the brittle fracture behavior of the ZSG composites. For sharp cracks which result in a $\alpha^{-1/2}$ singular stress field, the ZSG composites failure can be characterized by the Griffith fracture criterion based on fracture mechanics theory in terms of half crack length, α_{cr} [27]:

$$a_{cr} \approx \frac{{K_{IC}}^2}{\sigma^2 \pi} \quad (5)$$

α_{cr} is critical crack size for brittle fracture. σ, is the critical stress which will cause propagation of a crack-like flaw, α_{cr}. K_{IC}, is a material property referred to the toughness. That is to say, the Griffith fracture criterion describes the critical crack size that can occur without catastrophic crack propagation for brittle materials. Generally, the ZrB_2 based composites inevitably contained some flaws in the form of porosity, microcracks, impurity and so on. When the ZrB_2 based composites containing inherent flaws were subjected to thermal shock, thermal stress damage at tips of those preexisting flaws would be generated and hence catastrophic fracture would occur if thermal stress induced crack size to exceed critical crack size. In order to obtain an improved thermal shock resistance, it is necessary to have higher fracture toughness but lower flexural strength. That is, the fracture toughness and flexural strength synergistically affect the thermal shock resistance of the ZrB_2 based composites. This also supported theoretically the ZSG composites that have lower strength and superior thermal shock resistance compared with the ZrB_2–SiC composites. As shown in Table 2, the critical crack size of the ZSG composites was at least fourfold as large as the critical crack size of the ZrB_2–SiC composites based on the accepted strength of >800 MPa and toughness of <5.0 MPa $m^{1/2}$ for the ZrB_2–SiC composites [1,3,4]. In contrary to the mechanical properties of the ZSG composites, the thermal shock resistance increased with increasing graphite volume fractions.

4. Conclusions

The graphite flake toughened ZrB_2–20vol.%SiC composites were fabricated by hot-pressing. The relative density increased from 99.7 to 100.2% with the increase in the graphite volume fractions from 10 to 15 vol.% and the further increase in graphite volume fractions to 30 vol.% led to the reduction in the relative density to 97.2%. The mean grain size of ZrB_2 decreased as the graphite volume fractions increased at same sintering temperature. Furthermore, the mean grain size of ZrB_2 increased with the increasing sintering temperature. The flexural strength for ZSG15 composite did not decrease compared with that for ZSG10 composite, which was attributed to the refinement of ZrB_2 grains and the increase in the densification. The flexural strength drastically decreased from 367 to 277 MPa as the graphite volume fractions increased from 20 to 30 vol.%. Compared with the toughness of about 4.5 MPa $m^{1/2}$ for the ZrB_2–SiC composites, the ZSG composites have essentially higher toughness than do the ZrB_2–SiC composites due to their lower strength relative to the ZrB_2–SiC composites. The toughening mechanisms were related to the thermal residual stress. The presence of the thermal residual stress was confirmed by strain contours in SEM image and the maximum thermal residual stresses in interfaces of the graphite and other phases were evaluated to be about 1.4 GPa using Hsueh's formula.

Acknowledgments

This work was supported by the NSFC (90505015 and 50602010), the Research Fund for the Doctoral Program of Higher Education (20060213031).

References

[1] S.S. Hwang, A.L. Vasiliev, N.P. Padture, Mater. Sci. Eng. A 464 (2007) 216–224.
[2] S.Q. Guo, Y. Kagawa, T. Nishimura, H. Tanaka, Ceram. Int. 34 (2008) 1811–1817.
[3] S.M. Zhu, W.G. Fahrenholtz, G.E. Hilmas, J. Eur. Ceram. Soc. 27 (2007) 2077–2083.
[4] A.L. Chamberlain, W.G. Fahrenholtz, G.E. Hilmas, D.T. Ellerby, J. Am. Ceram. Soc. 87 (2007) 1170–1172.
[5] F.Y. Yang, X.H. Zhang, J.C. Han, S.Y. Du, J. Alloys Compd. 472 (2009) 395–399.
[6] W.B. Han, G. Li, X.H. Zhang, J.C. Han, J. Alloys Compd. 471 (2009) 488–491.
[7] X.H. Zhang, X.Y. Li, J.C. Han, W.B. Han, C.Q. Hong, J. Alloys Compd. 465 (2008) 506–511.

[8] L. Weng, X.H. Zhang, J.C. Han, W.B. Han, C.Q. Hong, J. Alloys Compd. 473 (2009) 314–318.
[9] Y. Wang, J. Liang, W.B. Han, X.H. Zhang, J. Alloys Compd. 475 (2009) 762–765.
[10] P. Zhang, P. Hu, X.H. Zhang, J.C. Han, S.H. Meng, J. Alloys Compd. 472 (2009) 358–362.
[11] W.M. Guo, G.J. Zhang, Y.M. Kan, P.L. Wang, J. Alloys Compd. 471 (2009) 502–506.
[12] X.H. Zhang, L. Xu, S.Y. Du, C.Y. Liu, J.C. Han, W.B. Han, J. Alloys Compd. 466 (2008) 241–245.
[13] S.K. Mishra, L.C. Pathak, J. Alloys Compd. 465 (2008) 547–555.
[14] Q.S. Zhu, X.L. Qiu, C.W. Ma, Carbon 37 (1999) 1475–1484.
[15] Z. Wang, C.Q. Hong, X.H. Zhang, X. Sun, J.C. Han, Mater. Chem. Phys. 113 (2009) 338–341.
[16] S.M. Zhu, W.G. Fahrenholtz, G.E. Hilmas, S.C. Zhang, Mater. Sci. Eng. A 459 (2007) 167–171.
[17] S. Baik, P.F. Becher, J. Am. Ceram. Soc. 70 (1987) 527–530.
[18] W.G. Fahrenholtz, Am. Ceram. Soc. 88 (2005) 3509–3512.
[19] X.H. Zhang, Z. Wang, X. Sun, W.H. Han, C.Q. Hong, Mater. Lett. 62 (2008) 4360–4362.
[20] H. Lee, R.F. Speyer, J. Am. Ceram. Soc. 86 (2003) 1468–1473.
[21] G.A. Gogotsi, Ceram. Int. 29 (2003) 777–784.
[22] K.T. Faber, A.G. Evans, Acta Metal. 31 (1983) 565–576.
[23] C.H. Hsueh, P.F. Becher, P. Angelini, J. Am. Ceram. Soc. 71 (1988) 929–933.
[24] D.K.L. Tsang, B.J. Marsden, S.L. Fok, G. Hall, Carbon 43 (2005) 2902–2906.
[25] T.N. Tiegs, P.F. Becher, J. Am. Ceram. Soc. 70 (1987) 109–114.
[26] J.W. Zimmermann, G.E. Hilmas, W.G. Fahrenholtz, Mater. Chem. Phys. 112 (2008) 140–145.
[27] D. Taylor, P. Cornetti, N. Pugno, Eng. Fract. Mech. 72 (2005) 1021–1038.